

# The gearless, grid-connected, 6-phase asymmetric wind turbine generator system

LESŁAW GOŁĘBIOWSKI<sup>1</sup>, MAREK GOŁĘBIOWSKI<sup>1</sup>,  
DAMIAN MAZUR<sup>1</sup>, MATTHIAS HUMER<sup>2</sup>

<sup>1</sup>Rzeszow University of Technology  
The Faculty of Electrical and Computer Engineering  
ul. Wincentego Pola 2, 35-959 Rzeszów, Poland  
e-mail: {golebiye/yegolebi/mazur}@prz.edu.pl

<sup>2</sup>Technische Universität Dortmund  
Lehrstuhl für Elektrische Antriebe und Mechatronik, Germany  
e-mail: matthias.humer@eon-energie.com

(Received: 05.12.2014, revised: 01.02.2015)

**Abstract:** In this paper a system of a grid side and a generator side converters, both working with a common capacitor, is presented. The 6-phase asymmetric inset-type SMPMSM generator is used. A large pole pair number of this generator enables a gearless wind turbine operation. The fundamental and 3rd harmonic cooperation is used to increase the generator performance. This is accomplished by means of the 3rd harmonic current injection. For that reason the generator side converter must have a neutral connection.

**Key words:** grid connected wind power turbine, three level converter, flying capacitors

## 1. Introduction

The investigated system is presented in Figure 1. This system is used to transfer the wind energy to the grid [1, 2]. Presented paper concerns the operation of the system designed in [3] and developed there quick control method based on the precalculated generator characteristics. Since the presented wind turbine-generator system is gearless, the generator is designed as a low and variable speed machine. It has a large number of pole pairs ( $p = 7$ ) and concentrated windings. It is a 6-phase asymmetric generator.

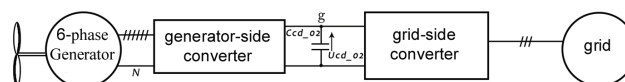


Fig.1. A simplified diagram of a system for grid connected wind power turbine

The control module allows an additional injection of third current harmonic. The tested system has following parameters: the generator rated power is 3.0 kW, its rated voltage is 141 V, voltage of the  $C_{cd02}$  capacitor is 400 V, grid phase voltage is 220 V. The dimensions of the tested generator can be found in [3].

## 2. Generator side converter

The three-level, seven-leg converter with flying capacitors  $C_{cd01}$  shown in Figure 2 is designed to supply the 6-phase asymmetric generator [4].

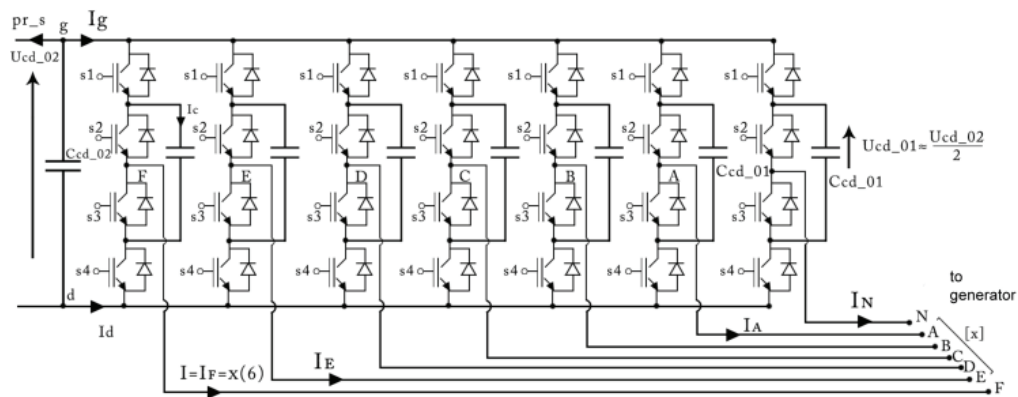


Fig. 2. The generator side three-level seven-leg converter with flying capacitors, [x] is the generator phase currents

In the investigated generator the 3rd harmonic current component flows in the neutral wire. Since the converter presented in Figure 2 has the neutral connection, the third harmonic current injection, which increases the generator performance, can be performed.

The investigated generator is driven by the wind turbine in a gearless system (Fig. 1). Therefore, it is designed as a low and variable speed machine with a large pole pairs number  $p$ . Since the number of the stator slots per pole pair is small the stator windings are concentrated. This kind of winding has a full spectrum of harmonics, with amplitudes approximately inversely proportional to their order. So the third harmonic of this system is large enough to be used for independent work and in cooperation with the fundamental harmonic [5, 6].

Considered here six-phase asymmetric generator is a simplification of the 12-phase symmetrical generator. In 12-phase generator 6 pairs of phases can be extracted. Each phase consists of a pair of identical two windings shifted by electrical  $180^\circ$  (facing each other). The tested six-phase asymmetric generator is created by connecting the windings in each such pair is in series. It can be said that it consists of two 3-phase windings, shifted by electrical  $30^\circ$  one from another, whose star points are connected. After the conversion of the generator windings to  $q-d$  coordinates, it turns out that the coordinates  $q_1-d_1$  are formed by fundamental harmonic and harmonics 11, 13, etc. ( $12 \cdot h \pm 1$ ). These higher harmonics produce unwanted moments.

However, their order is so high that their amplitude, as inversely proportional to their order, is small and undesirable moments are limited. This is the big advantage of the multiphase systems.

Coordinates  $q_3-d_3$  are created by third spatial harmonic, which is the fundamental harmonic for this coordinates. Unwanted harmonics in these coordinates are harmonics 9, 15 (overall  $12 \cdot h + 3, 12 \cdot h - 9$ ). The third harmonic, which is the fundamental harmonic in the coordinates  $q_3-d_3$ , is large enough to be able to be used for cooperation with the fundamental harmonic of the coordinates  $q_1-d_1$ . It can also, with appropriate control, work independently. In this manner the performance of the generator is increased and the torque pulsation are decreased.

The control of the generator side converter assures the existence of the 3rd harmonic current component. The magnitude of this component is depended on the magnitude of the fundamental component of this currents [3].

The generator phase currents, needed to achieve the generator set rotational speed are calculated [3,4]. The set rotational speed of the generator depends on the wind speed and system capabilities. The phase voltages of the generator are predicted for calculated currents [4]. Those voltages are then provided by the generator side converter (Fig. 2).

The generator side converter is powered by a capacitor  $C_{cd02}$ , which voltage is  $U_{cd02}$ . The voltage of the flying capacitors  $C_{cd01}$ ,  $U_{cd01}$  should be kept approximately equal to the half the voltage  $U_{cd02}$ . In each leg of the converter there are four valves  $s1, s2, s3, s4$ . It is assumed, omitting the dead time, that the valve state  $s3$  is the negation of the state of the valve  $s2$  ( $s3 = \sim s2$ ) and similarly  $s1 = (\sim s4)$ . Each of the phase currents, contained in the vector  $[x]$  and the current of the neutral wire  $I_N$ :

$$I_N = -\sum_{i=1}^6 x_i(t) \quad (1)$$

has its connection in the converter from Figure 2. There are four possible operating states of each converter leg, which are shown in Table 1.

Table 1. Possible operation states of each of the 7 legs of the converter from Fig. 2, ( $I_c$  is the charging current of capacitors,  $I$  is a current flowing to the stator phase,  $I_g, I_d$  are currents flowing out from nodes  $g$  and  $d$  – Fig. 2,  $U_{fd}$  is the voltage of phase relative to the node  $d$ )

State	s1, s2, s3, s4	$\begin{matrix} U_{cd\_01} \\ I > 0 \\ I < 0 \end{matrix}$	$I_g$	$I_d$	$I_c$	$U_{fd}$ , $U_{cd\_01} \approx 1/2 U_{cd\_02}$
1	1 1 0 0	doesn't change	$+I$	0	0	$U_{cd\_02}$
2	st23	$\uparrow \downarrow$	$+I$	0	$+I$	$U_{cd\_02} - U_{cd\_01} \approx 1/2 U_{cd\_02}$
3		$\downarrow \uparrow$	0	$+I$	$-I$	$U_{cd\_01} \approx 1/2 U_{cd\_02}$
4	0 0 1 1	doesn't change	0	$+I$	0	0

The 7th leg of the converter shown in Figure 2. creates the neutral voltage point

$$\frac{1}{2} U_{cd02}$$

in relation to node  $d$ . This converter leg operates only in 2nd or 3rd state. Both of these states together are called  $st23$ . The criterion for choosing between these states of work is the voltage across the flying capacitor and the need to keep this voltage, thanks to current  $I_c$ , at level of

$$U_{cd01} \approx \frac{1}{2} U_{cd02} .$$

Using the prediction of phase voltages of the generator [3, 4], it is assumed that in other converter legs each of the four states is possible.

The active time  $wzgl_w$  of each state (relative in the range of time step  $dt$ ), needed to achieve the required phase voltage is calculated. In context of the required voltage, the states 2 and 3 are treated equally as  $st23$  and the matrix of relative on-state times has 3 dimensions  $wzgl_w$  (1:3, 1:7). The second line  $wzgl_w$  (2, 1:7) is intended for states 2 and 3 ( $st23$ ). These states are distinguished by the need to keep the voltage at the flying capacitors  $C_{cd01}$  at half the voltage of the main capacitor  $C_{cd02}$ . The criterion for division of the state  $st23$  for states 2 and 3 is the direction of the phase current  $I$  and the attempt to reduce the absolute values of an error of the voltage (its deviations) on the capacitor  $C_{cd01}$ :

$$bl = \frac{1}{2} \cdot U_{cd02} - U_{cd01} \quad (2)$$

Table 1 allows to choose clearly between states 2 and 3. The relative active time of the selected state  $st23$  is determined by the voltage conditions: the converter must ensure proper phase voltage on the generator, calculated using prediction. Hence, the relative active time of this state  $st23$  is stored in the matrix  $wzgl_w$  (2, :). For the 7th leg of the converter, creating the zero point N, which should have the voltage  $U_{cd01} \approx 1/2 U_{cd02}$ , the relative time period of on-state of the state  $st23$  is 1. Node N is not directly connected to the node g or node d. We seek, however, to achieve good operating parameters of the converter at adequately small capacities  $C_{cd01}$ . Therefore, the voltage change on the capacity  $C_{cd01}$  during a given time step  $dt$  is limited to a preset value  $d_{UCgr}$  (eg 1 V). So, there is need to check whether, by given conditions, the change of voltage on the  $ii$ -th capacitor  $d_{UCa(ii)}$  is not greater than the predetermined value  $d_{UCgr}$ . The maximum on- time  $wzgl_{cz}$  for the condition of a limitation of voltage change on the capacitor to a preset value  $d_{UCgr}$  is calculated according to (3) ( $I$  is a phase current):

$$dt \cdot wzgl_{cz} = \left| \frac{d_{UCgr} \cdot C_{cd01}}{I} \right| . \quad (3)$$

When relative time  $wzgl_{cz}$  is smaller than the relative time  $wzgl_w(2, :)$ , which resulted from the voltage conditions, the time  $wzgl_w(2, :)$  should be reduced to the value  $wzgl_{cz}$ . The remaining difference in the relative times ( $wzgl_w(2, :) - wzgl_{cz}$ ) should be split in half for states 2 and 3. This separation does not change the voltage conditions (because both states 2 and 3 generate the same phase voltage). This does not change a charge of the capacitor  $C_{cd01}$  accumulated during on-state  $wzgl_{cz}$ , because both states 2 and 3 interact to the charge contrary and they cancel each other out, and the remaining relative time was split in half. However, this will change the current  $I_g$ , which is taken from the upper node g of  $C_{cd02}$  capacitor (in Fig. 2, the current  $I_d = -I_g$  will also change). Current  $I_g$  drawn by the generator system with converter

in Figure 2, is defined as the sum of currents flowing through the valves s1. As is apparent from Table 1, it is a current flowing during a state s1 with a value  $wzgl_{w(1, \cdot)} \cdot I(\cdot)$ , and the current flowing during a state s2, therefore  $wzgl_{w(2, \cdot)} \cdot I(\cdot)$ . When the increase of the capacitor voltage is limited to  $d_{UCgr}$ , this current should be updated. The reason for this is reduction of the relative time  $wzgl_{w(2, \cdot)}$  to the value  $wzgl_w$  while adding the states s2 and s3, with equal to each other relative on-time periods  $re$ :

$$re = \frac{wzgl_{w(2, \cdot)} - wzgl_w}{2} \tag{4}$$

If the initial state was equal to s2, the relative total flow of the current from the node g is equal to  $(wzgl_w + re/2) \cdot I$ , where  $I$  is the phase current of the generator. If the initial state was equal to s3, there the relative total flow of the current from the node g is equal to  $(re/2) \cdot I$ . A relatively long period of time step  $dt = 0.2$  [ms] was assumed. This allowed the described switching of the states. The time step equal to  $dt = 0.1$  [ms] was also tested successfully.

### 3. Grid side converter

Power drawn by the generator from the main capacitor  $C_{cd02}$  via generator side converter is equal to:

$$moc_{gc} = U_{cd02} \cdot I_g, \tag{5}$$

where  $U_{cd02}$  is the voltage across the capacitor. This voltage should be kept at a preset level  $U_{cd02st}$ . This is a task of the grid-side converter, shown in Figure 3.

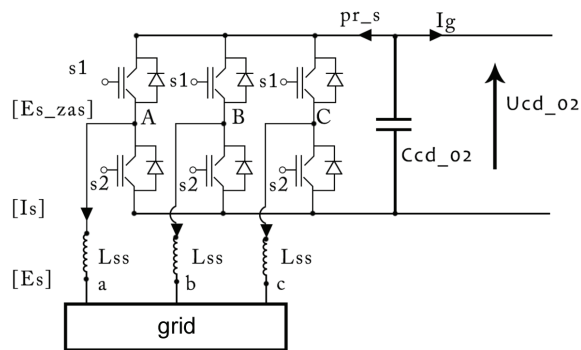


Fig. 3. Grid side converter transmitting energy from the generator (from capacitor  $C_{cd02}$ ) to the grid

This converter transmits power from the generator (from capacitor  $C_{cd02}$ ) to the grid. To ensure proper voltage on the capacitor, it should also be able to transmit energy in the other direction, from the grid to the generator. This task is performed by a two-level and three-leg

converter. Without taking into consideration the dead time between the commutations, it was assumed that the state of the valves  $s1$  is the opposite state of valves  $s2$  ( $s2 = \sim s1$ ).

An important element of the system is the inductance  $L_{ss}$ , ensuring continuity of grid currents  $[I_s]$ .

Voltage, which should be produced by the converter  $[E_{s_{zas}}]$  at terminals A, B, C can be written in the domain of complex numbers:

$$\underline{E}_{s_{zas}} = \underline{E}_s + j\omega \cdot L_{ss} \cdot \underline{I}_s, \quad (6)$$

where  $\underline{E}_s$  is a voltage across the terminals a, b, c.

To determine the phase relationships it can be assumed that the voltage of phase  $A$  of the grid is equal to:

$$e_{sA}(t) = E_{sm} \cdot \sin(\omega \cdot t), \quad (7)$$

where  $E_{sm}$  is the grid voltage peak amplitude, and  $\omega$  is the angular frequency.

It is assumed that given current of phase  $A$  is expressed by (8) (current arrow points into the grid).

$$i_{sA}(t) = I_{sm} \cdot \sin(\omega t) - |I_{sm}| \cdot \sin\left(\omega t - \frac{\pi}{2}\right). \quad (8)$$

The peak amplitude of the current active component (in phase with the voltage  $E_{sA}(t)$ ),  $I_{sm}$  is adjusted depending on the needs of the energy transmission. The second component of this current is a passive one. However, taking into account that the arrow of the current shown in Figure 3 points into the grid, the nature of the reactive power drawn from the network is inductive. This makes it easier to control and ensures its continuity. This can be seen in the vector diagram in Figure 4.

Current  $[I_s]$  (its active component) should compensate the power  $moc_{gC}$  drawn by the generator from capacitor  $C_{cd02}$ . At the same time it should ensure, that the voltage across the capacitor  $U_{cd02}$  is as close as possible to the preset value of  $U_{cd02st}$ . The relative error of this voltage is given by:

$$bl = \frac{U_{cd02} - U_{cdst}}{U_{cd02g} - U_{cd02st}}, \quad (9)$$

where  $U_{cd02g}$  is the assumed upper limit of the voltage:  $U_{cd02g} = 1.025 \cdot U_{cd02st}$ .

The maximal value of the active current component  $[I_s]$  consists therefore of two components:

$$I_{sm} = -\frac{moc_{gC}}{3 \cdot \frac{E_{sm}}{2}} + 0, 2 \cdot bl. \quad (10)$$

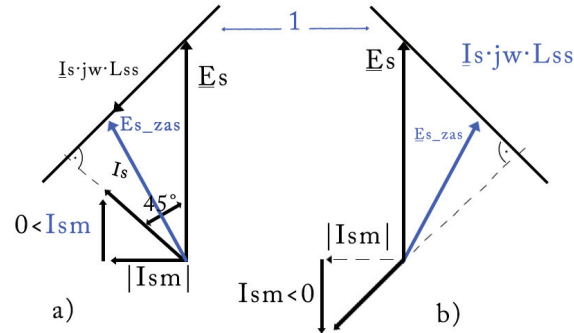


Fig. 4. Vector diagrams during the adjustment of the line converter of Fig. 3; lines 1 are the trajectory of the end of the regulation vector  $E_{s\_zas}$ ; a) when the active power is supplied to the network, b) when the active power is supplied to the generator, the current is inductive in nature (if one assumes that it flows out of the network, other than in Fig. 3)

As it can be seen from Figure 4, the amplitude of the voltage vector  $E_{s\_zas}$ , which has to be produced by the converter, changes its size when the end of the vector  $E_{s\_zas}$  moves along the regulation line 1. It is due to the capacitive component (inductive, if the grid currents has opposite direction to the direction shown in Figure 3.) of grid current  $[I_s]$ . For the converter control, the value of this voltage obtained from the prediction in the time domain is used:

$$es_{zas}(t+dt) = es(t+dt) + L_{ss} \cdot \frac{i_s(t+dt) - i_{s\_pop}}{dt}, \quad (11)$$

where  $(t+dt)$  is the time of the end of the time step  $dt$ ,  $es(t+dt)$ ,  $i_s(t+dt)$  is, adequately, the value of the grid voltage and the grid current for the end of the time step, and  $i_{s\_pop}$  is a known value of the grid current at the beginning of the considered time step. The maximal value of the grid voltage  $E_{sm}$  for which described control method works correctly is assumed as:

$$E_{sm} = \frac{1}{2} \cdot U_{cd02} - 5.0 [\text{V}]. \quad (12)$$

The value of the inductance taken for calculations was  $L_{ss}=10$  mH. As shown in Figure 4, this value determines the sensitivity of adjustment. It should also ensure continuity of grid current  $[I_s]$ . To ensure uniqueness of the control, the amplitude of the converter voltage  $E_{s\_zas}$  should decrease while the grid current  $[I_s]$  increases. This means that the amplitude of the voltage drop across the inductance  $L_{ss}$  must satisfy the relationship:

$$I_{sm\max} \cdot \omega \cdot L_{ss} < \frac{E_{sm}}{\sqrt{2}}, \quad (13)$$

where  $I_{sm\max}$  is the expected maximum value of  $I_{sm}$ , which should compensate the power consumed by the generator  $moc_{gC}$ .

Simulations were performed with the assumption that  $U_{cd02} = 400$  V,  $C_{cd01} = 100$   $\mu$ F,  $C_{cd02} = 200$   $\mu$ F.

In the presented above considerations the nature of the reactive power drawn from the grid is inductive. To achieve the capacitive power drawn, the control should be made according to the vector diagram of Figure 5.

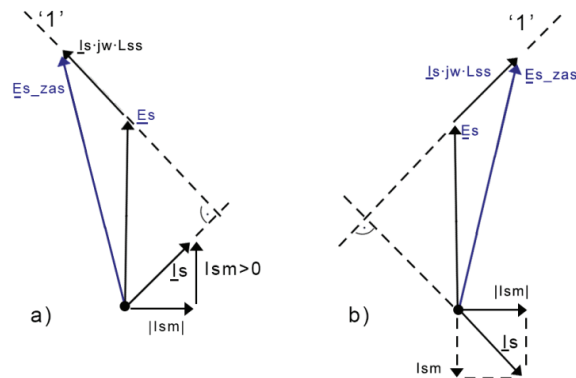


Fig. 5. Vector diagrams during the capacitive control of the network converter of Fig. 3 (current flows into the grid, according to Fig. 3); line '1' is a trajectory of the end of the control vector  $\underline{E}_{s_{zas}}$ ; a) the power is delivered to the network, b) the power is delivered to the generator

In this figure the active component of the grid current, depending on the direction of power flow, is marked by  $I_{sm}$ . In addition, the capacitive current  $|I_{sm}|$  is drawn from the grid (here marked as the current sent to the grid, as shown on Figure 3).

As seen in Figure 5,

$$|\underline{E}_{s_{zas}}| > |\underline{E}_s|.$$

The voltage

$$\underline{E}_{s_{zas}}$$

is created by the network converter from the voltage  $U_{cd02}$ . The maximal value of the grid voltage  $E_{sm}$  taken for simulations was:

$$E_{sm} = \frac{U_{cd02}}{2} - (I_N \cdot \omega \cdot L_{ss}) \cdot 2 = 162.32 \text{ [V]}. \quad (14)$$

The investigated system performs well when the active current component is not equal to the reactive component, and also when the reactive power drawn from the network is capacitive. The active current component is regulated depending on the wind speed and system capabilities, while the reactive current component is regulated according to the grid demands. The proposed system can work also with varying grid parameters. The measurements of the grid voltage amplitude and phase are necessary. Best performance of the system was achieved with the following component values (Fig. 2):  $C_{cd02} = 200$   $\mu$ F,  $C_{cd01} = 100$   $\mu$ F,  $L_{ss} = 2$  mH.



#### 4. Simulations of the tested system

In Figure 6 the dynamic waveforms of the system presented in Figure 1 are shown. This waveforms illustrates how the system is trying to reach the preset rotational speed  $\omega_{rad}$ . This speed depends from the measurements of wind speed, the capability of a wind turbine, and from the demand and constraints on produced power. Because the presented wind turbine system has no gears, it is a common speed for the generator and the turbine. The fast control method based on a quick searching of the precalculated characteristics, described in [3, 4], is used.

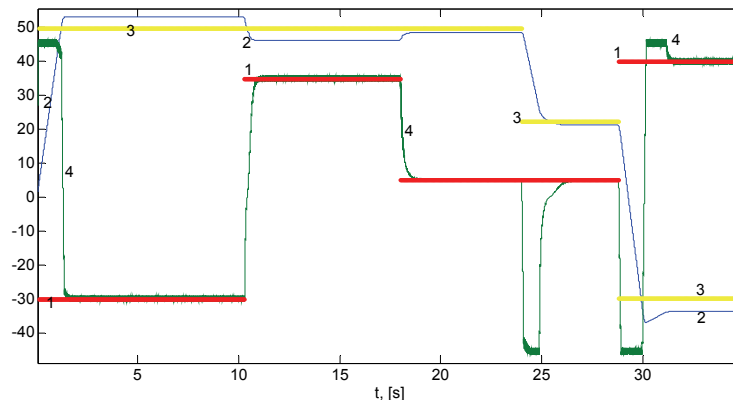


Fig. 6. Dynamic waveforms of the wind turbine - generator system presented in Fig. 1: 1) torque of the wind turbine, 2) actual speed of turbine-generator set, 3) preset speed  $\omega_{rad}$  resulting from measurements of wind speed, 4) electromagnetic torque produced by the generator, counteracting the torque generated by the wind turbine

The tested system creates the electromagnetic torque (4), which would counteract a torque of the turbine (1) in order to obtain the desired speed of the turbine-generator system (3).

Waveforms of stator phases currents, corresponding to the waveforms presented in Figure 6, are shown in Figures 7-8.

A shape of the stator phases currents illustrated in Fig. 8 (enlarged Fig. 7) is similar to a trapezoid. This indicates the participation of current components  $I_{q3}$ ,  $I_{d3}$ , appearing as the third time harmonic. The value of these currents  $I_{q3}$ ,  $I_{d3}$ , was conditioned during the control of components  $I_{q1}$ ,  $I_{d1}$ , with the factors  $k_{13}$ ,  $k_{24}$ . So the participation of these currents has been previously assumed as a third harmonic currents injection:  $I_{q3} = k_{13} \cdot I_{q1}$ ,  $I_{d3} = k_{24} \cdot I_{d1}$ , with the coefficients  $k_{13} = -0.1$ ,  $k_{24} = -0.3$ . It allows to take advantage of collaboration between primary (first) harmonic and the third harmonic, and of the action of the third harmonic alone [3, 4].

Selected coefficients ensure an existence of third harmonic currents in dependence on the first harmonic currents, what gives mutual enlargement of the torque and reduction of its pulsation [4].

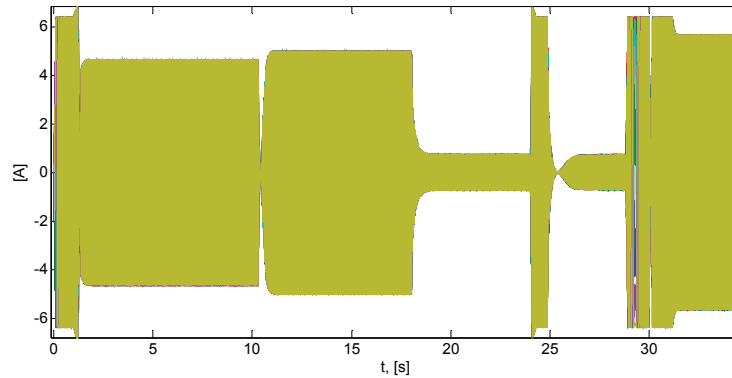


Fig. 7. Waveforms of phase currents of 6-phase asymmetric generator (corresponding to the waveforms shown in Fig. 6)

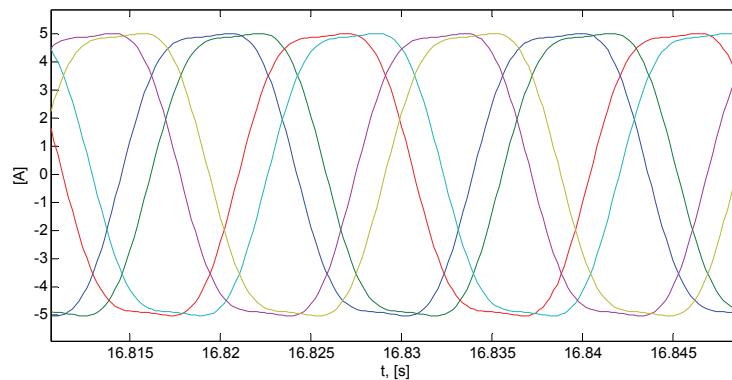


Fig. 8. Enlarged shape of the stator phase currents of Fig. 7

For the concentrated windings, which occur with many pole pairs  $p$  for low-speed machines, the share of the third harmonic is not negligible. It is produced by the third harmonic of the windings system and appears as the third harmonic of the magnetic induction in the air gap and in stator phases fluxes. After transformation to the  $q, d$  coordinates it appears as the main component of the  $q_3, d_3$  coordinates. The third time harmonic of the stator currents stimulates this  $q_3, d_3$  coordinate for action. Coefficients  $k_{13}, k_{24}$ , defining third harmonic currents shares in dependence on the first harmonic currents are not equal to each other, what indicates a shift of the  $q_3, d_3$  axis in the generator in comparison to the  $q_1, d_1$  axis. This shift is caused mainly by the chosen type of stator phases windings, as well as by the presence of permanent magnets.

The generator phases voltages waveform generated by the generator side converter is shown in Figure 9. The values of the required phase voltages are calculated as a voltage prediction by the controller. The generator's control was based on the quick search of the precalculated control characteristic presented in [3, 4].

Figures 10-11 show the currents  $I_g$  and  $pr_s$  drawn from the capacitor  $C_{cd02}$  of Figure 1 during operation of the system (presented wave forms correspond to the waveforms shown in Fig. 6). The current  $I_g$ , which is drawn by the generator converter from the capacitor  $C_{cd02}$ , has large pulsations. It is caused by the control of the generator's converter, which task is, besides

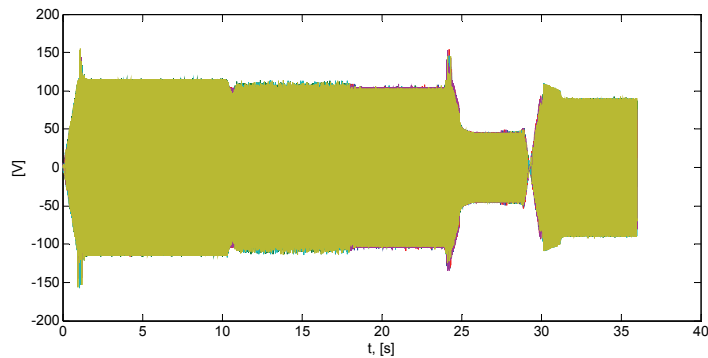


Fig. 9. Voltage supplying the generator phases, needed to provide dynamic waveforms of Fig. 6

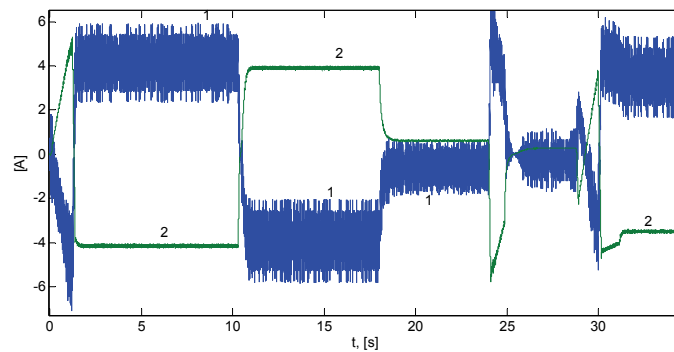


Fig. 10. Currents flowing from the capacitor  $C_{cd02}$  of Fig. 1: 1) current  $I_g$  drawn by the generator's converter of Fig. 2; 2) current  $pr_s$  drawn by the grid converter of Fig. 3

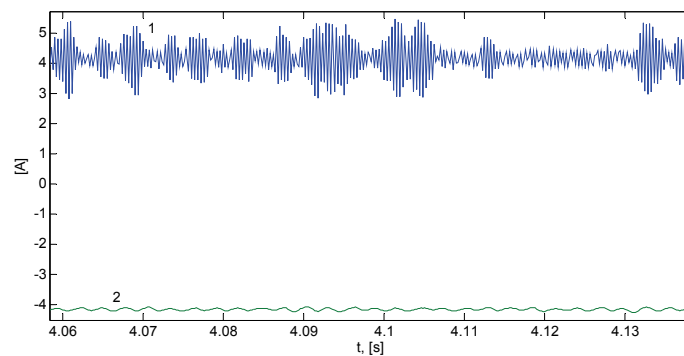


Fig. 11. Currents drawn from the capacitor  $C_{cd02}$  of Fig. 1: 1) current  $I_g$  and 2) current  $pr_s$  (enlarged part of Fig. 10)

providing the proper voltage on the phases of the generator, also to keep a set voltage on the  $C_{cd01}$  capacitors. This voltage should be approximately equal to half of the voltage on the main capacitor  $C_{cd02}$ . Current ripples  $I_g$  do not cause harmful effects, as they are integrated by the capacitor  $C_{cd02}$ .

Keeping a constant voltage  $U_{cd02}$  on the capacitor  $C_{cd02}$  is, however, the task of the network converter. Enlarged waveforms of the grid currents and of the phases voltages of the system from Figure 1 are shown in Figure 12. The inductive nature of the current drawn from the network was assumed. This is shown on the vector diagram of Figure 4.

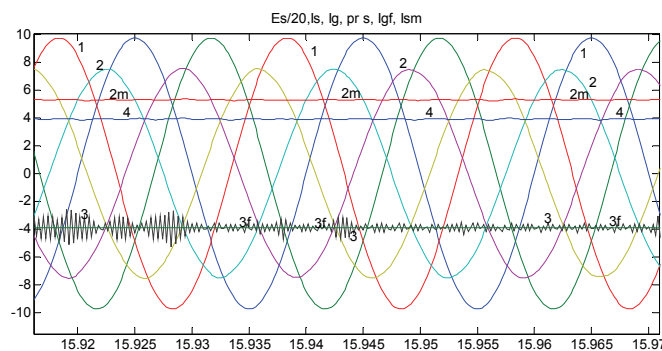


Fig. 12. Waveforms of: network phase voltages  $E_s/20$  (divided by 20) (line 1), the network current of inductive nature  $I_s$  (line 2), current  $I_g$  drawn from the capacitor  $C_{cd02}$  by the generator's converter (line 3), current  $pr_s$  drawn from the capacitor  $C_{cd02}$  by the network converter (line 4), the current drawn from the capacitor  $C_{cd02}$  by generator's converter after low pass filtering  $H(I_g)$  (line 3f), the envelope of network current  $I_{sm}$  (line 2m)

## 5. Conclusion

The described generator-side and grid-side, capacitor coupled, converters provide good operation of a gearless, grid-connected 6-phase asymmetric wind turbine generator. Thanks to the neutral connection of the generator-side converter it is possible to apply the 3rd harmonic current injection. This technique increases the performance of the generator. It should be noted that the use of the generators with an odd number of phases (5, 7, 9) reduces requirements for the generator converter, because neutral connection is not required then. In such a generator the third current harmonic flows in the phase wires, also the unwanted  $q_0$ ,  $d_0$  components are eliminated ( $q_0$ ,  $d_0$  components consists of 5th and 15th spatial harmonics). In the investigated 6-phase asymmetric generator the zero component of the currents flows in the phase wires. This component is the cause of the unwanted torque pulsations.

## References

- [1] Nahome Alemayehu Ayehunie, *MultiPhase Permanent Magnet Synchronous Generators for Off-shore Wind Energy System*. Norwegian University of Science and Technology Department of Electric Power Engineering (2011).

- [2] Levi E., Bojoi R., Profumo F. et al., *Multiphase induction motor drives – a technology status review*. IET Electric Power Applications 1(4): 489-516 (2007).
- [3] Mazur D., *Modeling and analysis of operation of machines SPMSM for winding turbines (in Polish)*. Oficyna Wydawnicza Politechniki Rzeszowskiej, Rzeszów (2013).
- [4] Kaźmierkowski M., Sędlak M., Styński S., Malinowski M., *Hierarchical Control of Four-Leg Three-Level Grid-Connected Converter for RES*. Wybrane Zagadnienia Elektrotechniki i Elektroniki (WZEE, CD), pp. 10-18 (2013).
- [5] Lubosny Z., *Wind Turbine Operation in Electric Power Systems*. (2003).
- [6] Levi E., *Multiphase Electric Machines for Variable Speed Applications*. Industrial Electronics, IEEE Transactions on 55(5): 1893-1909 (2008).